

# Novel Inspection Technique for Simultaneous Visualization of Two Waveforms Obtained by Two-Channel Simultaneous Monitoring

Tetsuya Yamamoto<sup>\*</sup>, Nobuyuki Toyama, Hidekazu Miyauchi, Hiroshi Tsuda

National Institute of Advanced Industrial Science and Technology (AIST), Tsukuba, Ibaraki, Japan

---

**Abstract** A novel inspection technique for the simultaneous visualization of two waveforms in two-channel simultaneous monitoring using two transducers is proposed. In this technique, the two-channel scattering waves as well as the incident waves from two directions are simultaneously visualized. Compared to the conventional inspection method that uses a single transducer, this technique not only contributes to intuitive and easy interpretation by making use of movies of scattering waves but also halves the inspection time. For a thin aluminum plate with a penetrating slit, scattering phenomena are visualized using two transducers placed at an angle of 90° to the target. For a thick plate with a small rectangular defect on the back surface, waveforms are visualized by two facing transducers. It is shown that the orthogonal positions of the two transducers relative to the target are important, particularly in testing for line-shaped cracks. This technique is a promising candidate for laser-excited ultrasonic inspection.

**Keywords** Pulsed Laser Scanning, Visualization, Simultaneous Monitoring, Non-Destructive Inspection

---

## 1. Introduction

In nondestructive inspection, ultrasonic wave testing has many virtues such as the ability to observe inside materials, easy handling, and compact equipment. Additionally, it is harmless to the human body compared to the other nondestructive inspection methods such as X-ray testing. Therefore, it is widely used as a nondestructive inspection method not only for transportation vehicles such as airplanes, trains, and automobiles, but also for large installations such as buildings and bridges [1-4]. In power and industrial plants, corrosion, cracks, and wall thinning in pipes caused by aging are other inspection targets for ultrasonic waves [5-7].

Although ultrasonic waves have excellent usefulness in nondestructive inspection, difficulties still remain, that is, the judgment of defects detected by echo signals depends only on the skill and expertise of the inspection experts. This is due to the complexity of the propagation behavior of ultrasonic waves in complex parts such as joints and curved surfaces. In welded joints in particular, waves propagate and repeat with multiple reflections and mode conversions. Consequently, even a professional inspector spends much time in distinguishing between defect echoes and false

echoes. Therefore, the development of easy and simple defect detection methods is needed.

Portable, easy-to-handle, and visually interpretable nondestructive inspection equipment using pulsed laser scanning has been developed [8-14]. The operating principle is that ultrasonic waves thermoelastically generated by scanning pulsed laser irradiation propagate through the specimen and are received by a transducer attached to the surface of the specimen. Based on the reciprocity principle of wave propagation, a time series of waveforms from all the laser irradiation locations are successively visualized as a movie in which the ultrasonic waves are transmitted from the transducer and travel through the specimen. Compared to the conventional inspection method in which a one-dimensional waveform (echo signal) is used for inspection, the visual inspection method making use of movies of scattering waves can be intuitively interpreted even by non-professional inspectors and is effective for avoiding misrecognition and overestimation. Moreover, this equipment has another advantage in that it is applicable to a specimen with a complicated surface, this is because the laser is not used as a vibrometer (interferometer) but only to excite ultrasonic waves, that is, the inspection is performed independent of the laser focus and laser incident angle to the specimen. As discussed above, this ultrasonic-wave inspection equipment has many advantages and can become a useful and effective tool to visualize ultrasonic-wave propagation behavior. This equipment can be used for studying material properties as

---

<sup>\*</sup> Corresponding author:

tetsuya.yamamoto@aist.go.jp (Tetsuya Yamamoto)

Published online at <http://journal.sapub.org/instrument>

Copyright © 2016 Scientific & Academic Publishing. All Rights Reserved

well as for other evaluations using ultrasonic waves, such as the evaluation of wave-scattering phenomena originating from defects, flaws, or damage to solid materials; evaluation of wave propagation in anisotropic materials; transducer evaluation; and validation of numerical analysis. It can also offer educational benefits through the visualization of ultrasonic wave propagation.

Thus far, the authors have mainly visualized wave propagation using a single transducer. Although two transducers were used in the two-channel equipment to realize quick measurement in some cases, the wave propagations from two transducers must be visualized separately by placing them individually in two different specimens, for example, two different T-tubes, with and without defects [8] or two aluminum or concrete blocks [13]. In another case in which we used two transducers, the transducers were placed at two different locations on the same skin/stringer specimen, and the waveforms from each transducer were visualized separately [8]. In the future, we expect the establishment of measurement techniques that are not dependent on the operator's skill and experience with regard to the choice of the transducer position and the laser irradiation surface. At the same time, the reduction of inspection time by half is desirable. It is a well-known fact that crack detection using a transducer placed parallel to a line-shaped crack is difficult due to the weak signals from the defect. This difficulty can be mitigated by using different directions and positions for the same specimen using multiple transducers. Using multiple transducers, not only in-plane diagnostics but also in-depth diagnostics can become possible. Furthermore, quick and efficient inspection would also be expected.

The phased array approach is well known for nondestructive inspection using multiple ultrasonic transducer elements. The Hitachi research group has developed three-dimensional (3D) imaging equipment using phased arrays to visualize flat bottom holes (FBHs) in a stainless steel test piece [15, 16]. The Toshiba group has also succeeded in obtaining clear images using a phased array [17, 18]. These approaches, in which the transducer plays a dual role of transmission and reception of ultrasonic waves, are not comparable to the laser-excited ultrasonic-wave technique. Moreover, in our laser scanning system, the receiving transducer can be moved separately on the specimen, while in the phased array, the densely arrayed elements are treated as a single component. In the technique using multiple transducers, called the sparse transducer array, multiple transducers can be placed separately, which is not possible with the phased-array transducer [19, 20]. In this case, however, one of the transducers is the emitter, and the remaining transducers in the array are receivers. In the sparse transducer array, the laser-excited ultrasonic waves are not used, and hence, this method cannot be compared with our proposed method. In an analogous technique using pulsed laser scanning, the research group of Toyota Central R&D Labs has reported the visualization of waveforms excited by laser irradiation

using multiple transducers [21-23]. They have recently proposed using multiple air-coupled transducers to receive the waveforms. This could become a promising candidate for the next generation of nondestructive, non-contact inspection and testing. However, with this system the evaluation is basically performed using only static images, and it differs from our inspection equipment mainly because ours produces movies (dynamic images). The research group of Chiba University placed three transducers concentrically at 120° intervals around the target and visualized the waveforms of laser-excited ultrasonic waves. Although snapshots of dynamic images (movies of scattering waves) as well as static images are presented in the literature [24], the received waveforms are visualized individually, as though a single transducer had been used three times at different positions for the measurement. In this case, although the measurements are recorded simultaneously, the movement of scattering waves from each transducer has to be checked individually, which is time-consuming. This visualization method using multiple transducers has already been researched and reported for the case of two transducers [8, 13]. To fully utilize the advantages of laser-excited ultrasonic wave inspection, a novel visualization technique using multiple transducers is required.

The present paper proposes a novel inspection technique of simultaneous visualization of movies of scattering waves with a two-channel simultaneous monitoring system. Compared to the conventional method using a single transducer, this technique allows intuitive and easy interpretation by making use of movies of scattering waves and also reduces the inspection time by half. First, the measurement system used to simultaneously record the waveforms using two transducers is presented. Second, the scattering movies of a thin aluminum plate with a penetrating slit are visualized using two transducers placed at an angle of 90° to the slit. In the thin aluminum specimen, two slit lengths are used: one is longer than the wavelength and the other is shorter than the wavelength. Third, as a more realistic model, a thick aluminum plate with a small defect on the back surface is visualized. In this measurement, waveforms from the two transducers facing each other are observed. Finally, a summary of this work is presented.

## 2. Visual Inspection Equipment and Measurement Procedures

Figure 1 shows the two-channel ultrasonic wave inspection equipment that uses pulsed laser scanning. The system configuration is essentially the same as that of the conventional system [8-13]. When the surface of a specimen is subjected to transient heating by pulsed laser irradiation, ultrasonic waves are produced as a result of surface motion from thermal expansion. The transient displacement of the material surface by thermal expansion generated by pulsed

laser irradiation is detected by two transducers of the same type (Japan Probe; transducer at oblique incidence, 2 MHz nominal resonance) at two different locations on the specimen. The waveform data (received signals) are stored in a personal computer as signed 8-bit integers via a preamplifier, filter, and high-speed analog-to-digital (A/D) converter. Using the reciprocity principle of wave propagation, a series of successive images is produced as an animation of the wave propagation, whereby ultrasonic waves are first transmitted from the transducer and then propagated through the solid material. In the low-noise preamplifier, filter, and A/D converter, which are present in the PCI bus of a personal computer, two channels were originally designed to meet component specifications, and therefore, two-channel simultaneous monitoring can be realized with these hardware components. LabVIEW<sup>®</sup> software synchronously controls the measurement components such as the laser, mirror, and A/D converter.

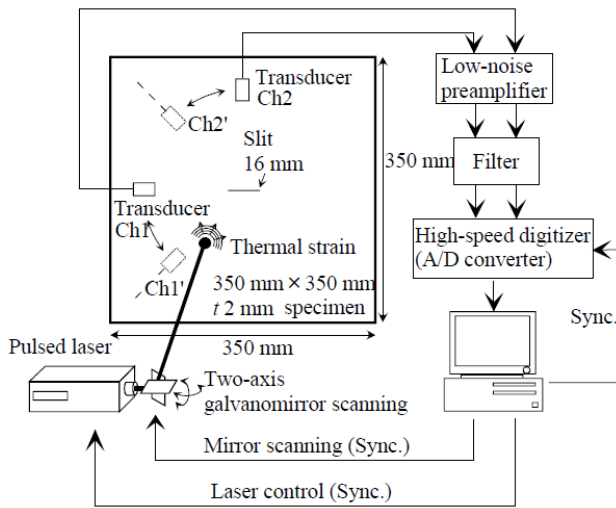


**Figure 1.** Two-channel ultrasonic wave inspection equipment using pulsed laser scanning

By using a power combiner/splitter such as T-connector between the two transducers and the low-noise preamplifier, single-channel measurement using two transducers can be realized, although the waveform data are mixed. In this paper, however, two waveforms are treated individually, as shown in Fig. 1, so that the waveforms are fed separately into each channel segment after measurement to enable their observation. Moreover, this is also because it is necessary to process the waveform in each channel so as to highlight the scattering waves visually by the subtraction technique [14].

For the specimens, two types of aluminum plates are used: thin and thick. Thin plates with a thickness of 2 mm with penetrating slits of two different lengths at their centers were used. The slits are 16 mm and 2 mm in length, and both had a width of 0.3 mm. In the thin plate, in order to observe only the 0th mode waves ( $S_0$  and  $A_0$  mode waves), the measurement was performed using a 700-kHz low-pass filter. Therefore, the phase velocities of the  $S_0$  and

$A_0$  mode waves are  $\sim 5100$  m/s and  $\sim 2500$  m/s, respectively, from the dispersion curve [25]. In this case, the wavelengths of the  $S_0$  and  $A_0$  mode waves are 7.3 mm and 3.6 mm, respectively, and in the thin aluminum plate, the one slit is longer and one is shorter than the wavelength. In the thick plate, on the other hand, the target to be detected is a small rectangular defect on the back surface. For the thick plate, two thicknesses were used, 20 mm and 10 mm. In the measurements using the thick plate, the filter was not connected (through mode).

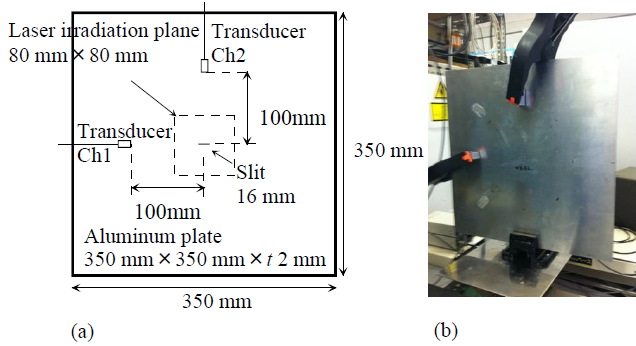
For the placement of two transducers, two types are tried: orthogonal position and facing position. When two transducers are placed at an angle of  $90^\circ$  to the target, since the main directions of two wavefronts transmitted from each transducer are orthogonal (independent), the scattering phenomena are easily recognizable and the judgement of defects is effortless. In the thin aluminum plate, therefore, the visualization was performed using two transducers placed orthogonally to the target. In the thick aluminum plate specimen, however, because the plate width is narrow and orthogonal placement of two transducers is difficult, the facing position was used.

### 3. Measurement Results and Discussions

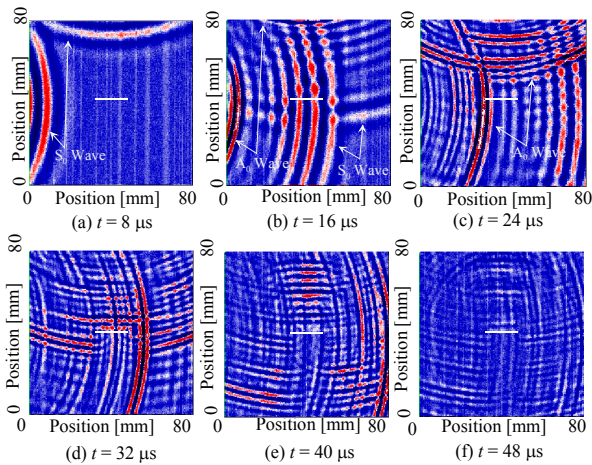
#### 3.1. Thin Plate with two Transducers Placed Orthogonally

Figure 2(a) shows the thin aluminum plate specimen with a 16-mm penetrating slit whose length is longer than the wavelength. Figure 2(b) shows a photograph of the thin aluminum plate specimen and the position of the two transducers. The dimensions of the plate are 350 mm  $\times$  350 mm  $\times$  2 mm, and the slit is at its center. The two transducers are placed orthogonally at 100 mm from the slit center, as shown in this figure (one is parallel to the slit and the other is perpendicular to it). The laser is scanned within the area of 80  $\times$  80 mm (200  $\times$  200 points) at a scanning pitch of 0.4 mm. The waveforms from the two transducers are stored simultaneously via the 700-kHz low-pass filter to measure only the plate waves of the 0th mode. This low-pass filter is always used in the experiments when the thin plate is used. Figure 3(a–f) show successive snapshot images of ultrasonic wave propagation at  $t = 8 \mu\text{s}$ , 16  $\mu\text{s}$ , 24  $\mu\text{s}$ , 32  $\mu\text{s}$ , 40  $\mu\text{s}$ , and 48  $\mu\text{s}$ , respectively. At  $t = 8 \mu\text{s}$ , the propagation of the faster  $S_0$  mode wave with a smaller amplitude from both left and upper sides are confirmed. At  $t = 16 \mu\text{s}$  and 24  $\mu\text{s}$ , the  $S_0$  wave passes through the slit. At  $t = 32 \mu\text{s}$ , the slower  $A_0$  mode with a larger amplitude passes through the slit, and until  $t = 48 \mu\text{s}$ , the reflection wave due to the  $A_0$  wave is observed mainly in the upward direction. Theoretically, when a plane wave is perpendicularly incident at the slit, a reflection wave from the slit's straight section as well as diffraction waves are generated at both slit edges [26]. In this figure, it is difficult to confirm the phenomenon because the amplitudes of the

incident wave and reflection wave from the slit's straight section are larger than the amplitude of the diffraction waves at both edges. Figure 3(g-i) show successive snapshot images of ultrasonic wave propagation after eliminating the incident waves using the subtraction technique at  $t = 32 \mu\text{s}$ ,  $40 \mu\text{s}$ , and  $48 \mu\text{s}$ , respectively. At  $t = 40 \mu\text{s}$ , faint edge diffraction waves are observed as two small hump-like waves generated at both edges.



**Figure 2.** Thin aluminum plate specimen with a penetrating slit and the positions of the two transducers



**Figure 3(a-f).** Successive snapshot images of ultrasonic wave propagation at  $t = 8 \mu\text{s}$ ,  $16 \mu\text{s}$ ,  $24 \mu\text{s}$ ,  $32 \mu\text{s}$ ,  $40 \mu\text{s}$ , and  $48 \mu\text{s}$

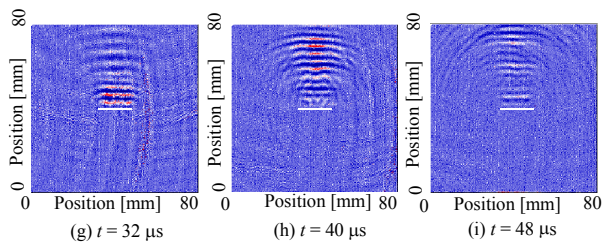


**Figure 3(g-i).** Successive snapshot images of ultrasonic wave propagation after the subtraction technique at  $t = 32 \mu\text{s}$ ,  $40 \mu\text{s}$ , and  $48 \mu\text{s}$

The same procedure is followed for 2-mm penetrating slit. The dimension of the plate is the same as the one with the 16-mm slit. The positions of the two transducers also remain the same, and the waveforms are similarly stored and visualized. Figure 4(a-f) show successive snapshot

images of ultrasonic wave propagation at  $t = 8 \mu\text{s}$ ,  $16 \mu\text{s}$ ,  $24 \mu\text{s}$ ,  $32 \mu\text{s}$ ,  $40 \mu\text{s}$ , and  $48 \mu\text{s}$ , respectively. At  $t = 8 \mu\text{s}$ , the propagations of the faster  $S_0$  wave with a smaller amplitude from both the left and upper sides are confirmed. At  $t = 16 \mu\text{s}$  and  $24 \mu\text{s}$ , the  $S_0$  mode wave passes through the slit. At  $t = 32 \mu\text{s}$ , a slower  $A_0$  mode wave with a larger amplitude passes through the slit, and until  $t = 48 \mu\text{s}$ , the reflection waves due to the  $A_0$  wave are confirmed to spread circularly. Figure 4(g-i) show the snapshots of successive images of ultrasonic wave propagation after eliminating the incident waves using the subtraction technique at  $t = 32 \mu\text{s}$ ,  $40 \mu\text{s}$ , and  $48 \mu\text{s}$ , respectively. In the case of the small slit, the reflection wave and edge diffraction waves generate a circular wavefront, which mainly propagates upward, perpendicular to the slit.

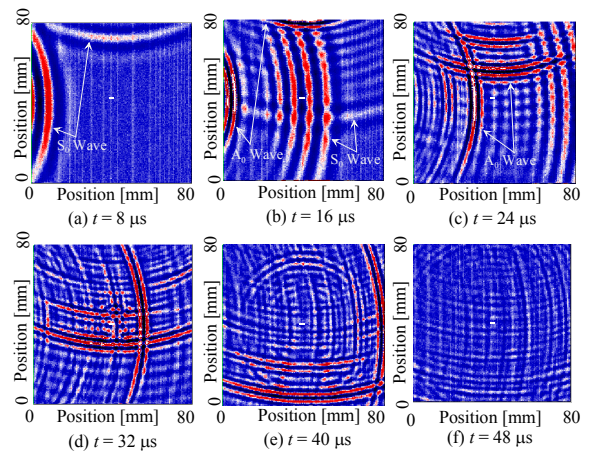


**Figure 4(a-f).** Successive snapshot images of ultrasonic wave propagation at  $t = 8 \mu\text{s}$ ,  $16 \mu\text{s}$ ,  $24 \mu\text{s}$ ,  $32 \mu\text{s}$ ,  $40 \mu\text{s}$ , and  $48 \mu\text{s}$

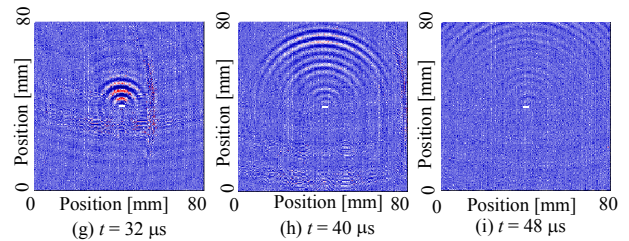


**Figure 4(g-i).** Successive snapshot images of ultrasonic wave propagation after the subtraction technique at  $t = 32 \mu\text{s}$ ,  $40 \mu\text{s}$ , and  $48 \mu\text{s}$

As the next step, the two transducers are placed orthogonally at angles of  $\pm 45^\circ$  to the slit as shown in Fig. 5(a). Figure 5(b) shows a photograph of the thin aluminum plate specimen with a 16-mm penetrating slit at its center and the positions of the two transducers. The two transducers are placed 120 mm from the slit center as shown in the figure. Figure 6(a-f) show successive snapshot images of ultrasonic wave propagation at  $t = 16 \mu\text{s}$ ,  $24 \mu\text{s}$ ,  $32 \mu\text{s}$ ,  $40 \mu\text{s}$ ,  $48 \mu\text{s}$ , and  $54 \mu\text{s}$ , respectively. At  $t = 16 \mu\text{s}$ , the wavefront of the  $S_0$  mode wave is on the penetrating slit. At the same time, the  $A_0$  mode waves are observed at the upper-left and lower-left corners. At  $t = 24 \mu\text{s}$ , the  $S_0$  mode

wave passes through the slit, and at  $t = 32 \mu\text{s}$  the wavefront of the slower  $A_0$  mode wave with the larger amplitude approaches the penetrating slit. At  $t = 40 \mu\text{s}$ ,  $48 \mu\text{s}$ , and  $54 \mu\text{s}$ , the diffraction wave at the far side edge due to the  $A_0$  mode wave is confirmed.

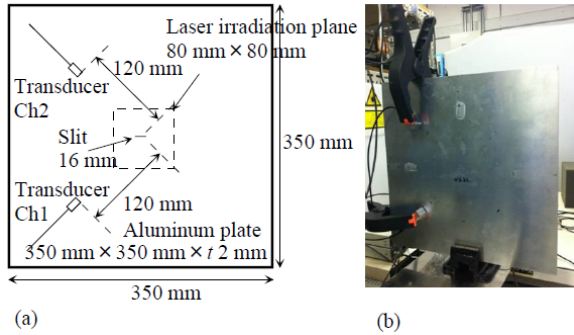


**Figure 5.** Thin aluminum plate specimen with a penetrating slit and the positions of the two transducers

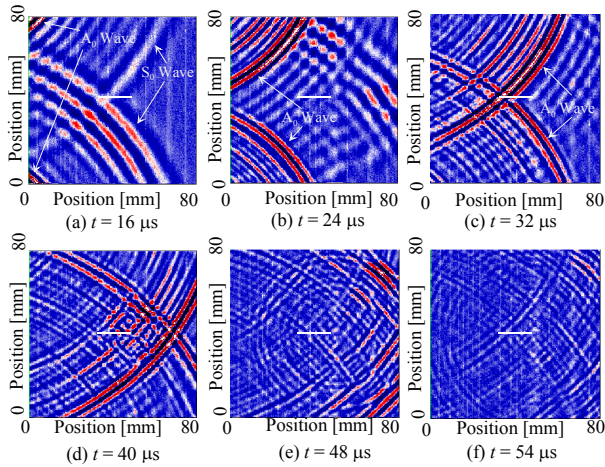


**Figure 6(a–f).** Successive snapshot images of ultrasonic wave propagation at  $t = 16 \mu\text{s}$ ,  $24 \mu\text{s}$ ,  $32 \mu\text{s}$ ,  $40 \mu\text{s}$ ,  $48 \mu\text{s}$ , and  $54 \mu\text{s}$

Similarly to the previous plate specimen, the thin aluminum plate specimen with the slit length of 2 mm on which the two transducers are placed  $\pm 45^\circ$  angles to the slit is tested. The two transducers are placed 120 mm from the slit center. The measurement condition is the same as in the previous case. Figure 7(a–f) show successive snapshot images of ultrasonic wave propagation at  $t = 16 \mu\text{s}$ ,  $24 \mu\text{s}$ ,  $32 \mu\text{s}$ ,  $40 \mu\text{s}$ ,  $48 \mu\text{s}$ , and  $54 \mu\text{s}$ , respectively. As shown in these figures, the reflection wave due to the faster  $S_0$  mode wave is hardly observed because the amplitude is weak. However, a clearer diffraction wave due to the slower  $A_0$  mode is confirmed at  $t = 40 \mu\text{s}$ ,  $48 \mu\text{s}$ , and  $54 \mu\text{s}$ .

In this sub-section, the authors observed scattering waves in the thin aluminum plate using two orthogonally placed transducers. As observed in the movies of scattering waves, it was found that even if the length of the defect is shorter than the wavelength, the scattering phenomenon can be confirmed sufficiently using the  $A_0$  mode wave without a subtraction technique [14]. In Figs. 3 and 4, it was notable

that the scattering wave was mainly observed only in the upward direction, that is, the incident wave from the transducer placed perpendicularly to the slit was mainly reflected, and the incident wave from the transducer placed parallel to the slit was not. This indicates that when the transducer is accidentally placed parallel to a line-shaped defect such as crack in nondestructive inspection, detection is difficult because of the weak reflection. However, by using two transducers orthogonally, the scattering phenomenon can be grasped at once. As shown in Figs. 6 and 7, even if the line-shaped crack is inclined relative to both transducers, it is correctly detected when the two transducers are orthogonally placed. In addition, by checking the movies that simultaneously visualize the waveforms from the two transducers, a quick inspection also can be realized (the inspection time is reduced by half). From the discussion above, the validity of this technique using two transducers was demonstrated.

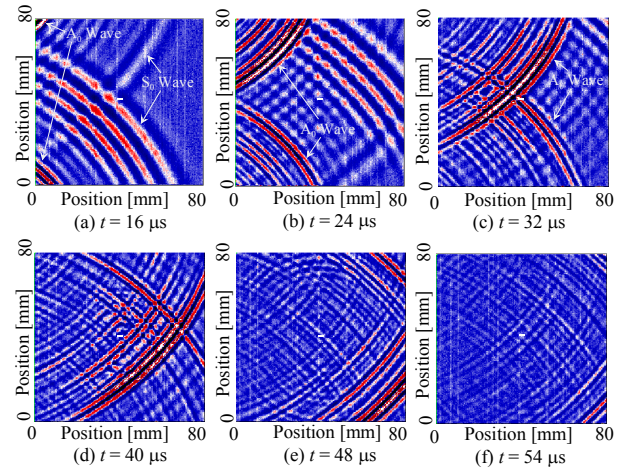


**Figure 7(a–f).** Successive snapshot images of ultrasonic wave propagation at  $t = 16 \mu\text{s}$ ,  $24 \mu\text{s}$ ,  $32 \mu\text{s}$ ,  $40 \mu\text{s}$ ,  $48 \mu\text{s}$ , and  $54 \mu\text{s}$

### 3.2. Thick Plate with two Transducers Facing each other

In the next step with a more realistic inspection model, two thick aluminum plate specimens with small rectangular defects on their back sides were tested. The two transducers are placed facing each other on opposite sides across the defect, and the waveforms are visualized. Figure 8(a) shows a 20-mm-thick aluminum plate specimen with a 2-mm rectangular defect on the back side at its center. Figure 8(b) shows a photograph of the thick aluminum plate specimen with the defect and the positions of the two transducers.

The dimension of the aluminum specimen is  $200 \text{ mm} \times 100 \text{ mm} \times 20 \text{ mm}$ . The two transducers are placed facing each other 50 mm from the defect as shown in the figure. The laser is scanned within an area of  $50 \times 50 \text{ mm}$  ( $200 \times 200$  points) at a scanning pitch of 0.25 mm. Figure 9(a–f) show successive snapshot images of ultrasonic wave propagation at  $t = 8 \mu\text{s}$ ,  $12 \mu\text{s}$ ,  $16 \mu\text{s}$ ,  $20 \mu\text{s}$ ,  $24 \mu\text{s}$ , and  $28 \mu\text{s}$ , respectively. The low-pass filter is not used in any of the experiments with the thick aluminum plates. As shown in this figure, at  $t =$

24  $\mu$ s, a faint reflection wave from the defect on the back side is confirmed.

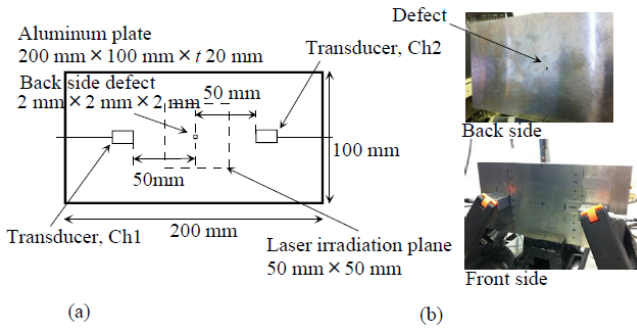


**Figure 8.** Thick aluminum plate specimen with a defect on the back side and the positions of the two transducers

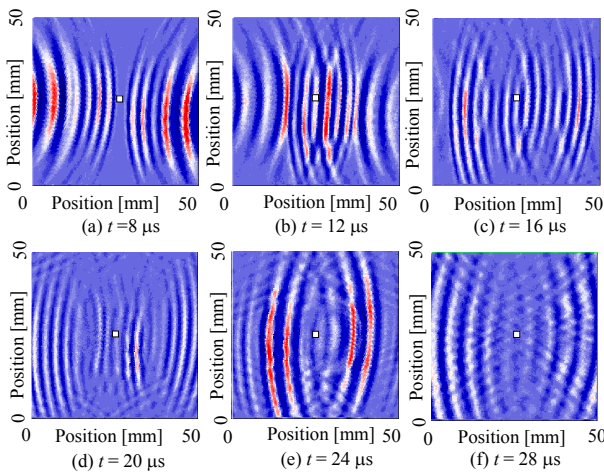


**Figure 9(a-f).** Successive snapshot images of ultrasonic wave propagation at  $t = 8 \mu$ s,  $12 \mu$ s,  $16 \mu$ s,  $20 \mu$ s,  $24 \mu$ s, and  $28 \mu$ s

Next the waveforms were measured in the 10mm-thick plate. The measurement condition is the same as the previous case. Similarly to the case of the 20-mm-thick plate, a faint scattering wave is observed at  $t = 20 \mu$ s and  $24 \mu$ s as shown in Figs. 10(a-f).

As discussed above, the scattering wave from the defect on the back surface was difficult to observe when the two transducers were placed facing each other. Therefore, the case using a single transducer in the same measurement condition is examined. Figure 11 (a) and (b) show the thick aluminum plate specimen with a rectangular defect on the back side and a photograph of the specimen with the position of the single transducer, respectively. These figures correspond to the case of the 20-mm-thick specimen, and the same procedure is also followed for 10-mm-thick specimen. Figure 12(a-f) show successive snapshot images of ultrasonic wave propagation in the 20-mm-thick specimen at  $t = 8 \mu$ s,  $12 \mu$ s,  $16 \mu$ s,  $20 \mu$ s,  $24 \mu$ s, and  $28 \mu$ s, respectively. Figure 13(a-f) show successive snapshot images of ultrasonic wave propagation in the 10-mm-thick specimen at  $t = 8 \mu$ s,  $12 \mu$ s,  $16 \mu$ s,  $20 \mu$ s,  $24 \mu$ s, and  $28 \mu$ s,

respectively. In both figures, at  $t = 24 \mu$ s and  $28 \mu$ s, the scattering waves from the defect on the back-side surface can be easily confirmed compared to the case when two facing transducers are used.

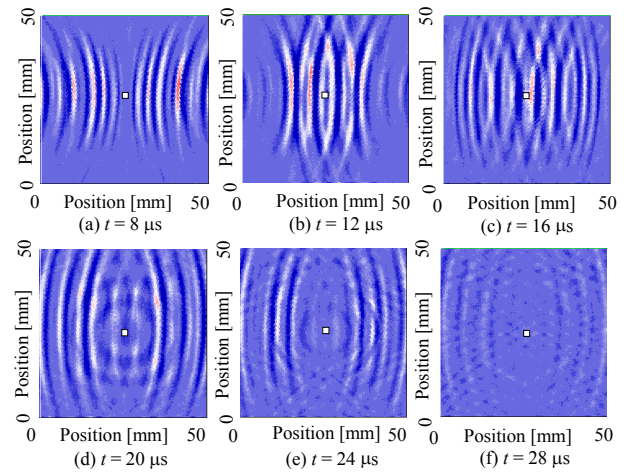


**Figure 10(a-f).** Successive snapshot images of ultrasonic wave propagation at  $t = 8 \mu$ s,  $12 \mu$ s,  $16 \mu$ s,  $20 \mu$ s,  $24 \mu$ s, and  $28 \mu$ s

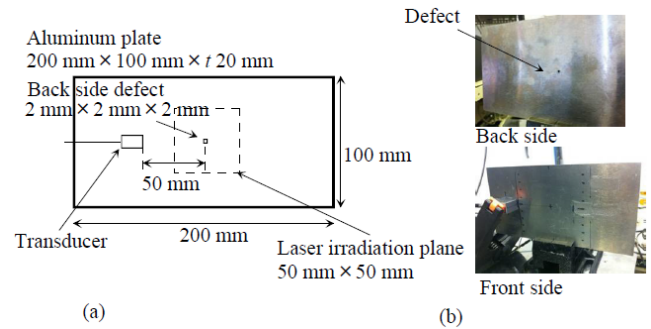


**Figure 11.** Thick aluminum plate specimen with a defect on the back side and the positions of the two transducers

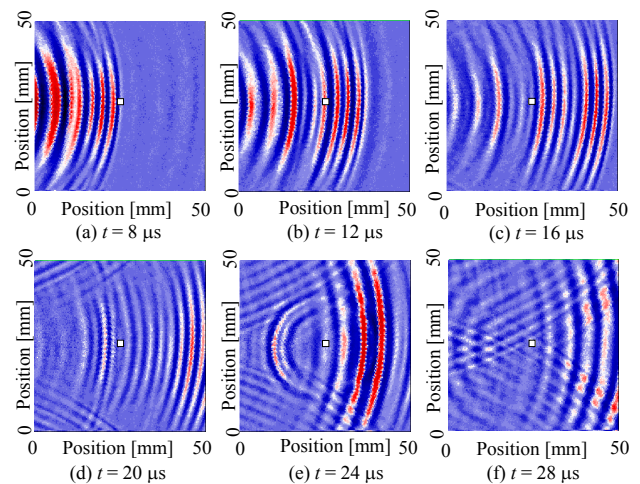


**Figure 12(a-f).** Successive snapshot images of ultrasonic wave propagation at  $t = 8 \mu$ s,  $12 \mu$ s,  $16 \mu$ s,  $20 \mu$ s,  $24 \mu$ s, and  $28 \mu$ s

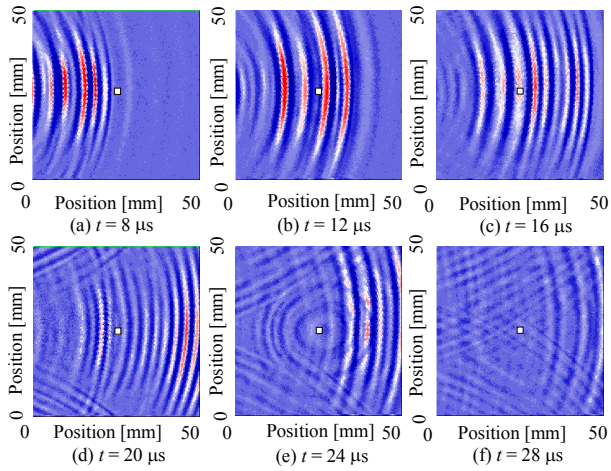


**Figure 13(a–f).** Successive snapshot images of ultrasonic wave propagation at  $t = 8 \mu\text{s}$ ,  $12 \mu\text{s}$ ,  $16 \mu\text{s}$ ,  $20 \mu\text{s}$ ,  $24 \mu\text{s}$ , and  $28 \mu\text{s}$

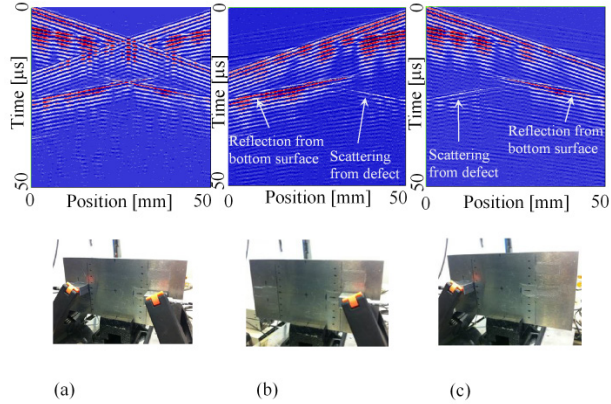


**Figure 14(a).** B-scope images of the two transducers on both sides of the 20-mm-thick plate, single transducer on (b) the right side and (c) the left side of the 20-mm-thick plate

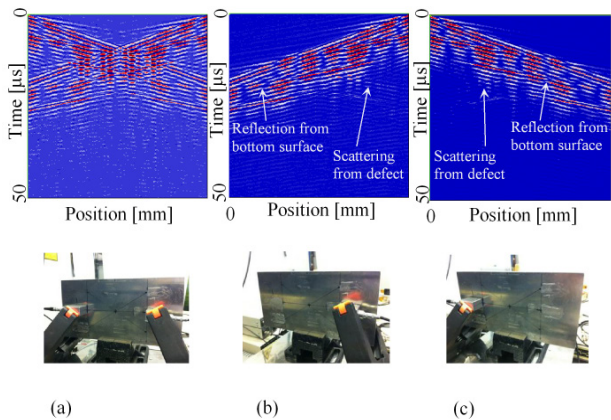


**Figure 15(a).** B-scope images of the two transducers on both sides of the 10-mm-thick plate, single transducer on (b) the right side and (c) the left side of the 10-mm-thick plate

In order to confirm the reason for the visual discrepancy, B-scope images of these ultrasonic waves are shown. Figure 14(a–c) show the B-scope images of two transducers on both sides of the plate and single transducers on the right

and left sides of the plate, respectively. The plate thickness is 20 mm. The B-scope image is expressed using the position and the time in horizontal and vertical axes, respectively, that is, the gradient in this figure represents the wave velocity. When the two transducers are used as shown in Fig. 14(a), the waves transmitted from each transducer are represented as two crossing gradients from both sides on the plate. When a single transducer is used as in Figs. 14(b) and (c), the wave transmitted from the transducer is represented only as the gradient from the side where the transducer is placed. The gradients starting from around the center in these figures are the reflection waves from the bottom surface including the scattering waves from the defect on its surface. Since the scattering wave from the defect spreads circularly, it travels in both (forward and backward) directions, while the reflection wave from the bottom surface propagates only into the one side (forward direction). When a single transducer is used, therefore, the scattering wave from the defect on the back surface can be confirmed clearly from the waves traveling in the backward direction. As shown in Fig. 14(a), however, when two transducers are used, the scattering wave from the defect on the bottom surface is overlapped with the reflection waves from the bottom surface making it difficult to observe. This tendency is particularly remarkable in the case of the 10-mm-thick specimen. Figure 15(a–c) show the B-scope images of two transducers on both sides of the plate and a single transducer on the right and left side of the plate, respectively, when using the 10-mm-thick aluminum plate. Since this plate is thinner than the one in the previous case, the reflection from the bottom surface occurs sooner than in the previous case of the 20-mm-thick plate. Therefore, various waves such as the incident waves, the reflection waves from the bottom surface, and the scattering waves from the defect on the bottom surface are in close proximity, and it becomes more difficult to distinguish between them.

## 4. Conclusions

A novel inspection technique for simultaneous visualization of two waveforms in two-channel monitoring equipment was proposed. First, the scattering phenomena in a thin aluminum plate with a penetrating slit were visualized using two transducers placed at an angle of  $90^\circ$  to the target. Second, for a more realistic model, the thick plates with small rectangular defects on their back surfaces were tested, and the waveforms from two transducers facing each other were visualized.

In the case of the thin plate, the scattering phenomena due to the  $A_0$  mode wave could be confirmed without using a subtraction technique. When the two transducers were placed orthogonal to the penetrating slit, that is, one was perpendicular to the slit and the other parallel, the scattering wave was mainly observed only in the upward direction, that is, the incident wave from the transducer placed perpendicular to the slit was mostly reflected, and the

incident wave from the transducer placed parallel to the slit was not. Furthermore, with a slit length of more than the wavelength, the diffraction waves at both edges together with the reflection wave from the slit's straight section were also confirmed. In the case using the thick plate, however, it was confirmed that the two facing transducers were not suitable for testing, because the scattering waves from the defect at the bottom surface overlapped with the reflection waves from the bottom surface. From the discussion above, in this simultaneous visualization technique, the placement of the transducer is particularly important, and arrangement of the two transducers orthogonal to the target is effective. It is difficult to observe scattering waves when the transducer is accidentally placed parallel to a line-shaped defect such as crack. Even in such a case, scattering waves can be easily and reliably observed by visualizing two waveforms measured by two transducers placed orthogonally.

Inspections using more than three transducers, not only for in-plane diagnostics but also for in-depth diagnostics using multiple transducers, and extremely small defect detection using multiple transducers are left for future studies.

## ACKNOWLEDGEMENTS

This research was partially supported by a Grant-in-Aid for Scientific Research (C), (Grant No. 25420426) of the Japan Society for the Promotion of Science (JSPS).

## REFERENCES

- [1] Rose, J. L. and Soley, L. E., Ultrasonic guided waves for anomaly detection in aircraft components, *Material Evaluation* (2000), pp. 1080–1086.
- [2] Goglio, L. and Rossetto, M., Ultrasonic testing of adhesive bonds of thin metal sheets, *NDT & E International*, Vol. 32 (1999), pp.323–331.
- [3] Liang, M. T. and Wu, J., Theoretical elucidation on the empirical formulae for the ultrasonic testing method for concrete structures, *Cement and Concrete Research*, Vol. 32, No. 11 (2002), pp. 1763–1769.
- [4] Rolander, D. D., Phares, B. M., Graybeal, B. A., Moore, M. E. and Washer G. A., Highway Bridge Inspection: State-of-the-Practice Survey, *Transportation Research Record*, Vol. 1749, (2001), pp. 73–81.
- [5] Rose, J. L., Guided wave nuances for ultrasonic nondestructive evaluation, *IEEE Transactions on Ultrasonics, Ferroelectrics and Frequency Control*, Vol. 47, No. 3 (2000), pp. 575–583.
- [6] Sposito, G., Ward, C., Cawley, P., Nagy, P. B. and Scruby, C., A review of non-destructive techniques for the detection of creep damage in power plant steels, *NDT & E International*, Vol. 43, No. 7 (2010), pp. 555–567.
- [7] Naus, D. J., Oland, C. B., Ellingwood, B. R., Graves III, H. L. and Norris, W. E., Aging management of containment structures in nuclear power plants, *Nuclear Engineering and Design*, Vol. 166, No. 3 (1996), pp. 367–379.
- [8] Takatsubo, J., Generation laser scanning method for visualizing ultrasonic waves propagating on 3-D objects (in Japanese), *Journal of the Japanese Society for Non-Destructive Inspection*, Vol.57, No.4 (2008), pp. 162–168.
- [9] Takatsubo, J., Wang, B., Tsuda, H. and Toyama, N., Generation laser scanning method for the visualization of ultrasounds propagating on a 3-D object with an arbitrary shape, *Journal of Solid Mechanics and Materials Engineering*, Vol. 1, No.12 (2007), pp. 1405–1411.
- [10] Yashiro, S., Takatsubo, J. and Toyama, N., An NDT technique for composite structures using visualized Lamb-wave propagation, *Composites Science and Technology*, Vol. 67 (2007), pp. 3202–3208.
- [11] Lee, J., Takatsubo, J., Toyama, N. and Kang, D., Health monitoring of complex curved structures using an ultrasonic wavefield propagation imaging system, *Measurement Science and Technology*, Vol. 18 (2007), pp. 3816–3824.
- [12] Yashiro, S., Takatsubo, J., Miyauchi, H. and Toyama, N., A novel technique for visualizing ultrasonic waves in general solid media by pulsed laser scan, *NDT & E International*, Vol. 41 (2008), pp. 137–144.
- [13] Takatsubo, J., Development of nondestructive inspection technologies using laser ultrasonic visualizing method (in Japanese), *Inspection Engineering*, Vol.15, No.1 (2010), pp. 24–30.
- [14] Takatsubo, J., Miyauchi, H., Urabe, K., Tsuda, H. and Toyama, N. and Wang, B., Imaging of scanning waves from rear slits by using a synchronizing differential method with laser UT (in Japanese), *Journal of Solid Mechanics and Materials Engineering*, Series A, Vol. 75, No. 750 (2009), pp. 211–218.
- [15] Kitazawa S., Kono, N., Baba, A. and Adachi Y., A three-dimensional phased array ultrasonic testing technique, *10th European Conference on Non-Destructive Testing*, (2010).
- [16] Kitazawa, S., Odakura, M., Otani, K. and Adachi, Y., Advanced inspection technologies for energy infrastructure, *Hitachi Review*, Vol. 59, No. 3 (2010), pp. 111–115.
- [17] Arai, R., Yamane, N., Isobe, H. and Hamajima, T., Large-scale 3D ultrasonic inspection system (in Japanese), *Toshiba Review*, Vol. 62, No. 8 (2007), pp. 57–61.
- [18] Abe, M. and Karasawa, H., Matrixeye portable 3D ultrasonic inspection system (in Japanese), *Toshiba Review*, Vol. 60, No. 4 (2005), pp. 48–51.
- [19] Michaels, T. E. and Michaels, J. E., Sparse ultrasonic transducer array for structural health monitoring, *Review of Quantitative Nondestructive Evaluation*, vol. 23 (2004), pp. 1468–1475.
- [20] Zhao, X., Gao, H., Zhang, G., Ayhan, B., Yan, F., Kwan, C. and Rose, J. L., Active health monitoring of an aircraft wing with embedded piezoelectric sensor/actuator network: I. Defect detection, localization and growth monitoring, *Smart Materials and Structures*, vol. 16 (2007), pp. 1208–1217.

- [21] Hayashi, T., Murase, M. and Kitayama, T., Defect visualization by a scanning laser source technique (in Japanese), *Proceedings of the Japanese Society for Non-Destructive Inspection Spring Conference*, (2010), pp. 69–70.
- [22] Hayashi, T., Murase, M. and Kitayama, T., Full non-contact and fast defect imaging using scanning laser source technique (in Japanese), *Proceedings of the 19th Symposium on Ultrasonic Testing*, (2012), pp. 87–92.
- [23] Hayashi, T., Murase, M. and Kitayama, T., Defect imaging technique using a scanning laser source, *Review of Progress in Quantitative NDE*, Vol. 30, (2010), pp. 713–719.
- [24] Hattori, T., Watanabe, T., Hu, N. and Liu, Y., Damage area evaluation using a new and simple signal-processing algorithm in the ultrasonic wave propagation visualization technique (in Japanese), *Transactions of the Japan Society of Mechanical Engineers, Series A*, Vol. 78, No. 795, (2012), pp. 1506–1517.
- [25] Rose, J. L., *Ultrasonic waves in solid media*, Cambridge, Cambridge University Press, Chap.8, (1999).
- [26] Furukawa, A., Saitoh, T. and Hirose, S., Wave scattering analysis by a crack using convolution quadrature boundary element method (in Japanese), *Proceedings of the Conference on Computational Engineering and Science*, Vol.17, (2012).